Structural Engineering and Mechanics, Vol. 20, No. 1 (2005) 45-67
DOI: http://dx.doi.org/10.12989/sem.2005.20.1.045

'Modularised' Closed-Form Mathematical model for predicting the bracing performance of plasterboard clad walls

Y. L. Liew†

Department of Civil and Environmental Engineering, The University of Melbourne, Victoria 3010, Australia

E. F. Gad‡

School of Engineering and Science, Swinburne University of Technology, P.O. Box 218, Hawthorn, Victoria 3122, Australia

C. F. Duffield‡†

Department of Civil and Environmental Engineering, The Australian Centre for Public Infrastructure, Melbourne University Private, Victoria 3052, Australia

(Received May 7, 2004, Accepted February 15, 2005)

Abstract. This paper presents a new approach to predict the racking load-displacement response of plasterboard clad walls found in Australian light-framed residential structures under monotonic racking load. The method is based on a closed-form mathematical model, described herein as the 'Modularised' Closed-Form Mathematical model or MCFM model. The model considers the non-linear behaviour of the connections between the plasterboard cladding and frame. Furthermore, the model is flexible as it enables incorporation of different nailing patterns for the cladding. Another feature of this model is that the shape of stud deformation is not assumed to be a specific function, but it is computed based on the strain energy approach to take account of the actual load deformation characteristics of particular walls. Verification of the model against the results obtained from a detailed Finite Element (FE) model is also reported. Very good agreement between the closed form solution and that of the FE model was achieved.

Key words: light-framed structures; plasterboard; gypsum; timber construction; shear resistance; bracing; mathematical modelling.

1. Introduction

In Australia, walls with nominally fixed plasterboard for non-bracing walls have been indirectly used for lateral bracing. The recently superseded Australian National Timber Framing Standard

† PhD Candidate, Corresponding author, E-mail: y.liew@civenv.unimelb.edu.au
‡ Senior Research Fellow, E-mail: egad@swin.edu.au
‡† Associate Professor, E-mail: c.duffield@civenv.unimelb.edu.au

(AS1684-1992) assumed that such plasterboard lined walls provide 40% and 20% of the lateral bracing required for single and double storey houses, respectively. In 1999, the AS1684 was revised and renamed the Residential Timber-Framed Construction Standard. The revised standard allows the contribution of plasterboard lined walls to provide up to 50% of the lateral bracing required for both single and double storey houses. In addition, this standard explicitly nominates a bracing contribution of 0.45 kN/m for walls with nominally fixed plasterboard cladding on one side and 0.75 kN/m for walls with cladding on both sides. There is no provision in the current Australian and New Zealand Gypsum Plasterboard Standard (AS/NZS2588-1998) for specific product testing to quantify the bracing performance of plasterboard. As a result, plasterboard manufacturers frequently conduct full-scale isolated wall racking tests to verify the bracing capacity of their newly developed products and systems. Such testing is usually an expensive and time-consuming exercise. A new test has been developed that is simple, cost effective and enables the assessment of the bracing performance of plasterboard during manufacture on the production line. The development and verification of this new test is reported in Liew *et al*. (2002). To further streamline the process to control the bracing performance of plasterboard, a spreadsheet-based analytical model has been developed. This model has the ability to translate the results of a fastener-to-sheathing connection (shear connection) test, which is typically simple and repeatable, into full-scale isolated wall racking test results. The focus of this paper is on the development and verification of this analytical model.

Numerical models for predicting the load-displacement response of isolated racking walls have been studied by researchers over the past five decades, e.g. Neisel and Guerrera (1956), Neisel (1958) and Welsch (1963). The models developed by these researchers were empirical relationships between the wall racking strength and the lateral nail resistance of individual fasteners obtained from testing. Such an approach is limited to the adopted testing procedures and conditions, hence, the models have significant limitations.

In the forty years since these initial empirical relationships were developed, a number of models have been developed to describe the racking performance of walls in more detail, particularly the load-displacement response. These models can be classified into two main categories, namely mathematical models that allow for closed-form solutions and Finite Element (FE) models. Closed-form mathematical models have been somewhat simplistic as they describe the overall response of a wall of a given configuration without comprehensively analysing each component of the wall. Indeed, the closed-form mathematical modelling approach was adopted by Tuomi and McCutcheon (1978), Easley *et al.* (1982), Gupta and Kuo (1985), McCutcheon (1985), Patton-Mallory and McCutcheon (1987), Murakami *et al.* (1999) and Salenikovich (2000) to model wood-based sheathings (e.g. plywood and OSB) clad walls typically used in the United States. Contrary to closed-form mathematical models, FE models are more complicated but versatile since they are capable of producing detailed analysis of all wall components with different configurations, such as different boundary conditions and nail spacing, provided that the components and connections of the wall are defined appropriately. Researchers including as Foschi (1977), Itani and Cheung (1984), Gutkowski and Castillo (1988), Dolan (1989), White (1995), Kasal *et al.* (1994) and Folz and Filiatrault (2001, 2002) successfully developed racking wall models using FE formulations. These models were essentially developed and verified for wood-based sheathing clad walls rather than for plasterboard clad walls, typically used in Australian construction. Plasterboard clad walls exhibit other failure modes which are not often observed in OSB or plywood clad walls as discussed in the following section.

2. Knowledge gaps of available analytical models

It has been established from a review of the above mentioned literature that both types of analytical modelling approaches have varied capabilities of predicting the racking performance of isolated walls. Even though simple, given the correct assumptions on the deformation of the frame and sheathing, closed-form mathematical models are able to predict the lateral load-displacement response of walls with reasonable accuracy. In contrast, the formulation of FE models is considerably more sophisticated than that of closed-form mathematical models and hence a higher level of programming expertise and computational power are required. The FE models have the ability to provide detailed information on the performance of various components of a wall along with the overall load-displacement response.

Commercially available FE packages used for structural analysis generally require users to undertake special training in order to acquire competent modelling skills. Moreover, such FE packages can be a significant expense for users. Closed-form mathematical models, however, can be easily programmed using commonly available spreadsheet program such as Microsoft Excel, fulfilling the demand for straightforward and cost effective computer programs to perform regular design computations.

Although the closed-form mathematical models and FE models developed by past researchers are able to predict the load-displacement response of walls subjected to lateral loading with acceptable degree of accuracy, the majority of these models were developed and verified for use on walls clad with plywood or wood-based materials. Furthermore, in these models, it was assumed that the sheathings are fixed vertically with uniform nailing configurations. These models cannot be applied to study the performance of plasterboard clad walls commonly found in light-framed residential structures built in Australia because:

- unlike plywood and OSB sheathings, plasterboard exhibits a different failure mode and load-slip characteristic at the connections located around the cut edges of plasterboard compared to those within the board (field), presented in Fig. 1, (terminology of typical Australian plasterboard is

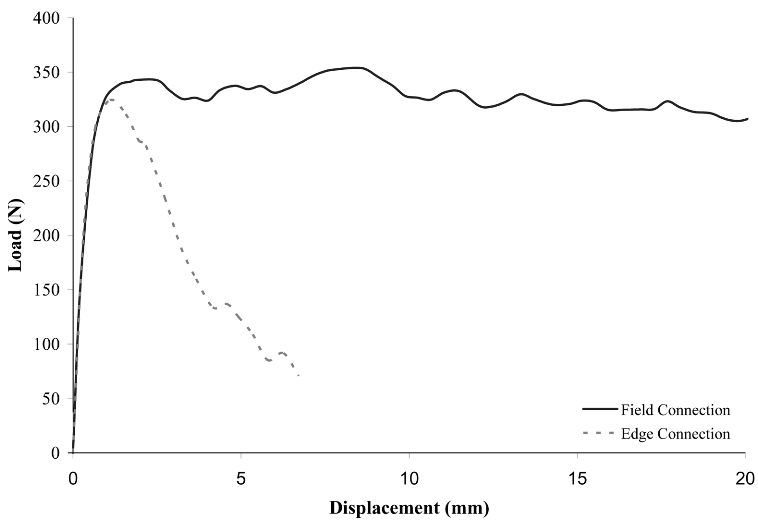

Fig. 1 Typical load-slip curves from shear connection tests

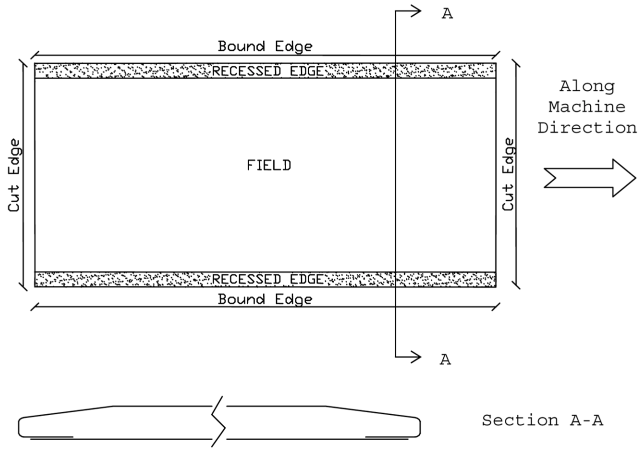

Fig. 2 Typical plasterboard with recessed edges used in residential construction in Australia

defined in Fig. 2). Hence, existing models which assume the same load-slip characteristics for all the fasteners regardless of their locations are unsuitable for accurate modelling.

- it is common in Australia to have more fasteners located along the vertical edges of plasterboard compared with those in the field and along the top and bottom plates. Hence, any closed-form mathematical model to be applicable in Australia must allow different fastener spacing for the vertical edges, plates and intermediate studs (refer to Fig. 3). Most of the existing closed-form mathematical models do not allow for this flexibility and cannot be easily modified.
- the available closed-form mathematical models assume different shapes of stud deformation such as parallelograms assumed by Tuomi and McCutcheon (1978); sinusoidal shape (S-shape) by Gupta and Kuo (1985); and vertical cantilevers by Salenikovich (2000). To date, the S-shape stud deformation presented by Gupta and Kuo (1985) seems to be the most reasonable assumption as it is observed in most full-scale isolated wall racking tests. However, the model developed by Gupta and Kuo (1985) assumed the same deformation for all the studs in a wall.

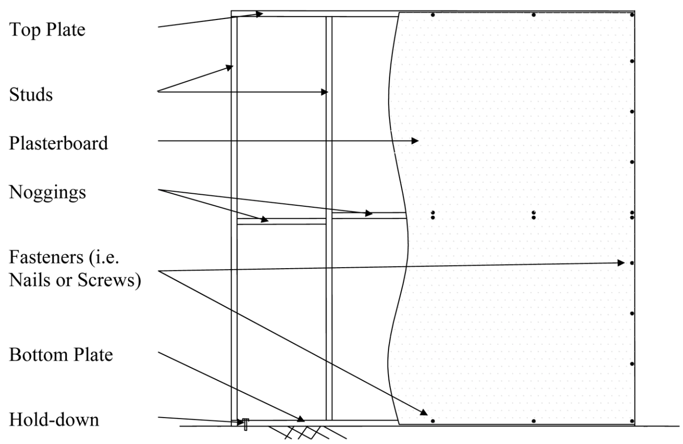

Fig. 3 Components in a typical plasterboard clad wall

This assumption is not applicable for plasterboard clad walls because the edge studs typically undergo more deformations than that of the intermediate studs due to a different failure mode (tear out) of plasterboard.

- in Australia, wall plasterboard is usually glued to ceiling plasterboard via ceiling cornices. The ceiling cornices prevent the plasterboard from rotating but allow lateral (in-plane) movement. This type of wall behaviour is not observed in isolated wall racking test since the cornices and skirting boards are omitted. Furthermore, boundary restraints such as skirting board and cornice provide significant additional racking resistance to the plasterboard clad walls as they prevent out-of-plane buckling of plasterboard and also restrict the relative rotation between the plasterboard and the frame (Reardon 1990 and Gad 1997). Hence, analytical models which are based on the behaviour of isolated walls without such restraints would not be appropriate in predicting the response of walls which are in use.

Based on the above mentioned unique features of plasterboard clad walls, it can be concluded that a new closed-form mathematical model, which incorporates the effects of the cornices and skirting boards, needs to be developed for plasterboard clad walls typically found in Australian residential structures.

3. 'Modularised' Closed-Form Mathematical model

The capability of assigning different load-slip characteristics of shear connections and thus, the effects of the fastener locations on the bracing performance of the walls into a predictive model is important for walls clad with plasterboard. This is particularly the case where the shear connections at the cut edges of plasterboard are substantially weaker than that of the recessed edges and field. Furthermore, due to the weakness of the cut edges, the deformations of the studs at the vertical edges of plasterboard clad walls would be different than those of the intermediate studs. Such difference in stud deformations is also not considered by the closed-form mathematical models currently available.

Another limitation in most of the available closed-form mathematical models is that they have very little flexibility for modifying the fastener spacing along the wall perimeter and the intermediate studs. In addition, these available models assume a constant shape of stud deformation. A more generic approach for determining the shape of stud deformations is thus required.

To overcome the above limitations, a 'Modularised' Closed-Form Mathematical (MCFM) model has been developed in this study. The MCFM model employs the strain energy approach to model the non-linear behaviour of plasterboard clad walls, similar to Gupta and Kuo (1985). However, instead of solving all the unknowns such as force, stud deformation and sheathing deformation by using a final expression (closed-form formulation), the MCFM model divides the formulation into two modules as described below and presented in the flowcharts shown in Figs. 4 and 5.

The first module is designed to establish the deformations of the studs relative to the plasterboard at each incremental displacement and the information obtained is then stored into a database. It is important to note that this model does not have pre-assumed stud deflection profile. Instead, the deformations of all the studs are generated using a simple sub-model which calculates the deformation of each single stud according to the stiffness of the stud and the load-slip characteristics of the shear connections on the stud.

In the second module, using the stud deformation information compiled in the database, the energy stored in each individual shear connection and the energy stored in each stud of the wall can then be determined based on the load-slip characteristics of the shear connections and the assumed elastic properties of timber, respectively. This enables the ‘modularised’ formulation to incorporate the different load-slip characteristics of shear connections into the model. Next, the load-

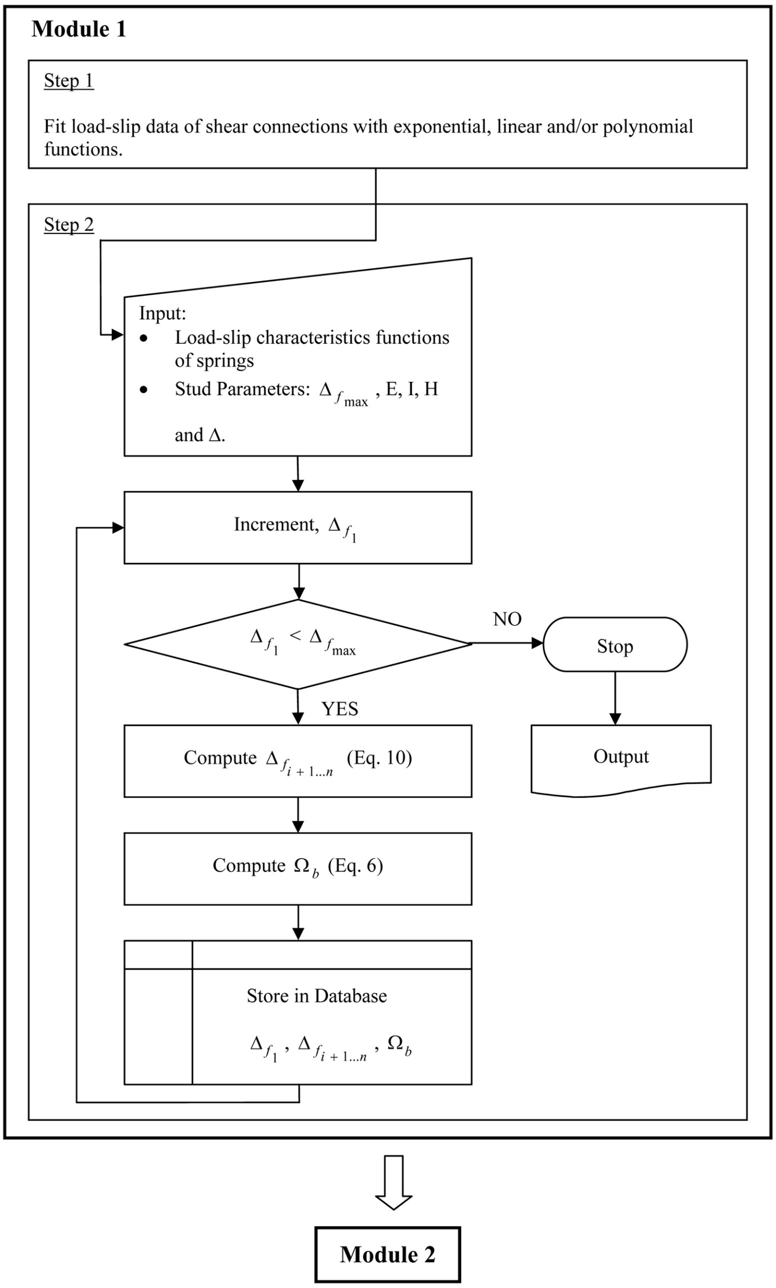

Fig. 4 Flowchart showing Module 1 of the MCFM Model

displacement response of the wall model due to frame deformation and nail slip is determined through an iterative procedure. Finally, the additional racking displacement caused by shear in the plasterboard is added to the frame deformation and the nail slip obtained previously in order to calculate the actual displacement. The details of these two modules are discussed in the following sections.

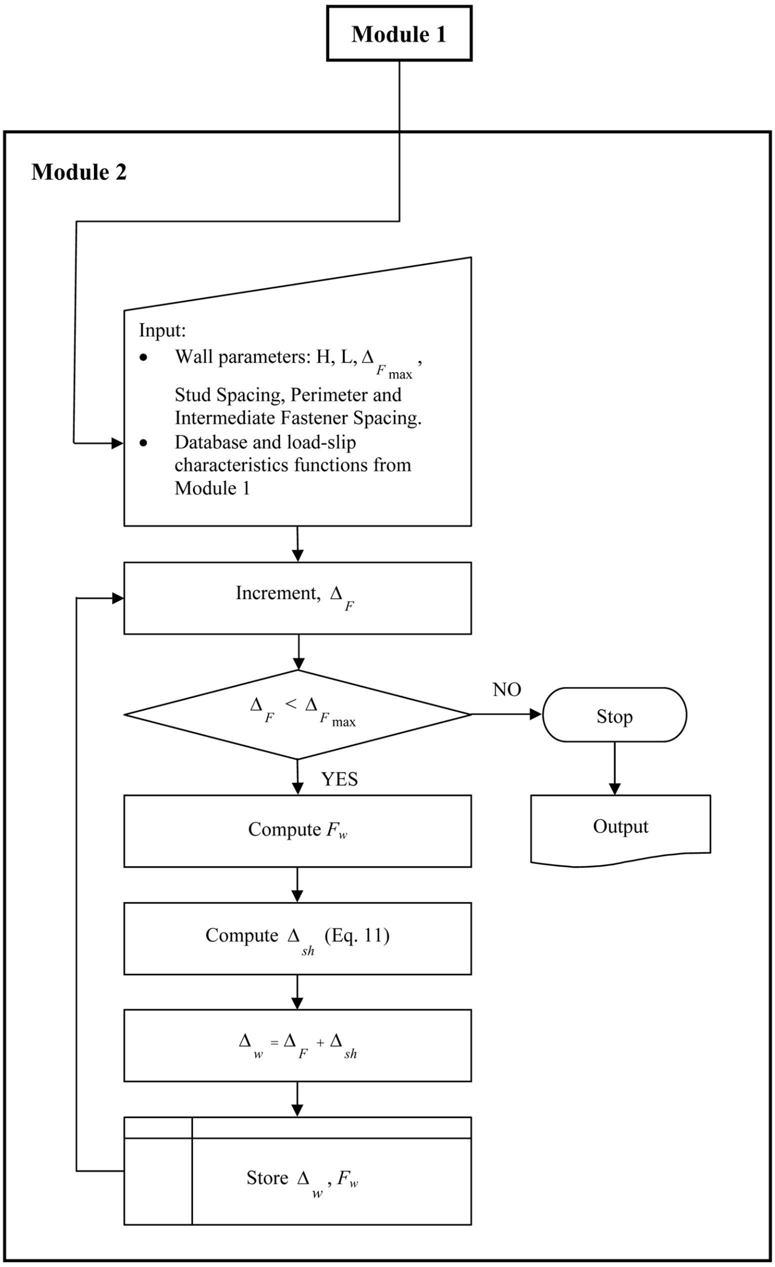

Fig. 5 Flowchart showing Module 2 of the MCFM Model

4. Assumptions for MCFM model

Incorporation of the effects of the cornices and skirting boards in the developed MCFM model reflects common practice for Australian residential structures. This enhancement makes verification of the model more complex as experimental results of full-scale isolated wall racking tests cannot be directly compared with the results from the MCFM model because it is almost universal that full-scale isolated wall racking tests do not include such components. Thus, in order to validate the results from the MCFM model, a verified FE model was used. The FE model was validated against the experimental results and later modified by incorporating the boundary conditions, in which the

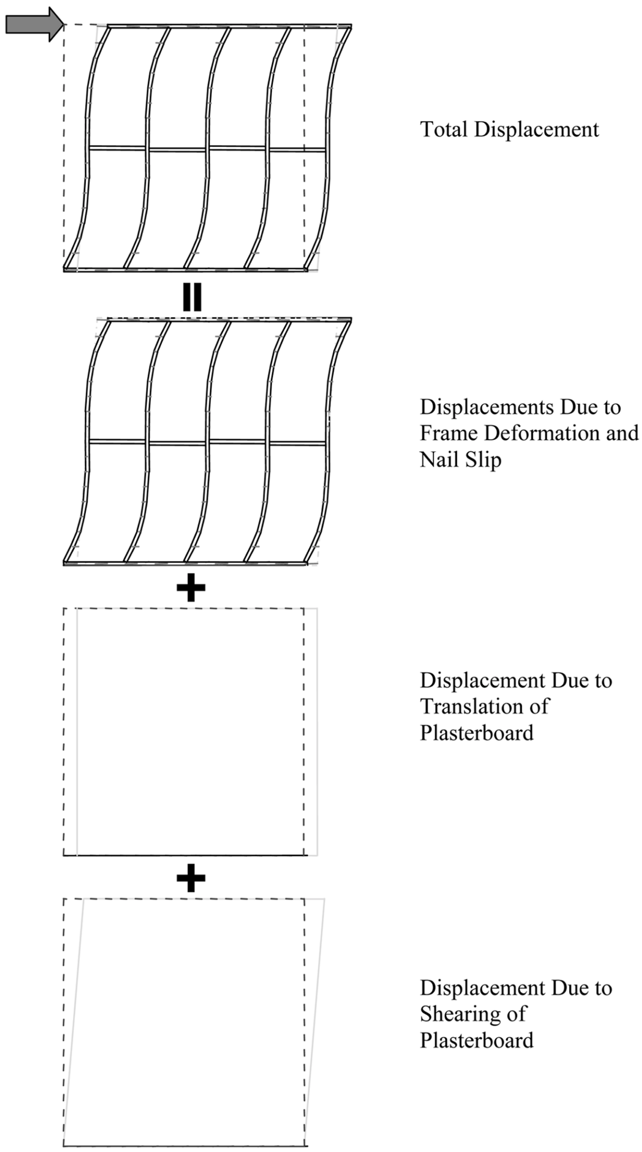

Fig. 6 Displacements of frame, plasterboard and nails when plasterboard clad wall is subjected to racking load

effects of the cornice, that prevent the plasterboard from rotating relative to the frame, and the skirting board, that prevent the out-of-plane buckling of the plasterboard at the bottom, were included. The modified FE model was then used to validate the MCFM model. This FE model was previously verified against experimental results by Gad *et al*. (1999).

In order to develop an accurate model using the strain energy approach, the ability to quantify the deformation of a wall is vital. The results from the FE model identified that the total displacement of a plasterboard clad wall under racking load is attributed to:

a) displacements due to frame deformation and nail slip
b) translation of plasterboard, and
c) shearing of plasterboard.

These attributes are illustrated in Fig. 6. When a racking load is applied to the wall, the studs deform in symmetrical S-shape and cause the nail to slip relative to the plasterboard. At the same time, the racking load which is transferred through the shear connections initiates the translation and shear deformation of the plasterboard. The MCFM model has taken these contributions into account when deriving the total displacement of plasterboard clad walls.

Another important finding obtained from the FE analysis was that the studs of the plasterboard clad wall deformed symmetrically about the mid height, while the plasterboard translated at half the maximum deformations of the studs. This finding allowed the MCFM model to be simplified by determining the bending strain energy and the strain energy due to slip in the shear connections of each stud at half the height of the wall. By doubling the amount of these strain energy and adding the strain energy due to slip in the shear connections on both the top and bottom plates, the total strain energy of the wall can then be found.

The following are the additional assumptions were adopted for the development of the MCFM model:

- Noggings are not included in the MCFM model as no shear connections are normally located at the noggings of plasterboard clad wall.
- The top plate is modelled as a rigid beam. Hence, when load or displacement is applied to the top plate, all the shear connections at the top plate would move at the same displacement. In addition, although the tip of the five studs would move at the same displacement as that of the top plate, each stud is assumed to deform independently based on the spacing of fasteners between the cladding and stud and also the shear capacity of these fasteners (note, edge fasteners are weaker as described in Section 2).

5. Module 1: Establish database for stud deformation and bending energy

The steps employed in Module 1 for predicting the shape of stud deformations and stud bending strain energy with different fastener spacing configurations as well as different types of plasterboard are presented in detail in the following two steps.

5.1 Step 1: Fitted curves for load-slip characteristics of shear connections

In general, two types of shear connection can be found in plasterboard clad walls, namely connections in the middle of the wall (field connections) and connections at the left and right edge of the wall (edge connections). These two types of connections have very different load-slip

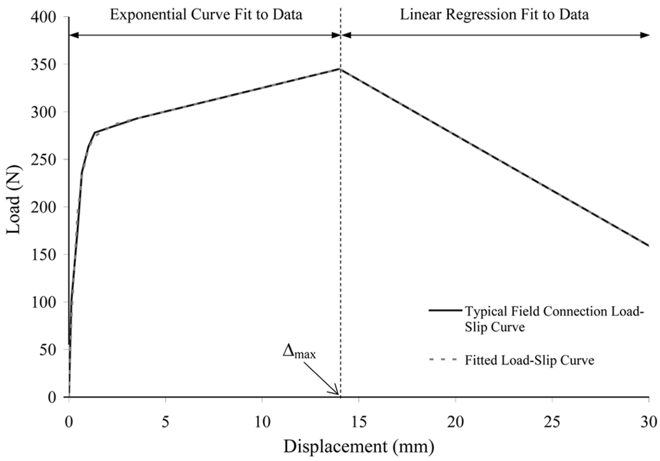

Fig. 7 An example of fitted load-slip curve for a field shear connection

characteristics and hence fitted using different functions. Typical fitted curves for filed and edge connections are shown in Figs. 7 and 8, respectively. Note that fitting of field connection is done in two sections.

As depicted in Fig. 7, a typical load-slip curve of field shear connections can be fitted using a least squares regression analysis up to the peak load based on the exponential function proposed by Foshi (1974):

$$F_{sc} = (A + B\Delta_f)\left(1 - \exp\left(-\frac{C}{A}\Delta_f\right)\right) \qquad (\Delta_f \le \Delta_{max}) \tag{1}$$

where F_{sc} = Shear connection force
Δ_f = Displacement due to slip in shear connection
Δ_{max} = Displacement at peak load
A, B and C are the variables obtained through fitting the data using a least squares regression method. The physical meanings of these variables correspond to that of the parameters described in Foshi (1974) as p_0, p_1 and k, respectively.

The descending slope after the peak load can be expressed by a simple linear function:

$$F_{sc} = M\Delta_f + N \qquad (\Delta_f > \Delta_{max}) \tag{2}$$

where F_{sc} = Shear connection force
Δ_f = Displacement due to slip in shear connection
M and N are the variables obtained through fitting the data using a linear regression method.

In situation where the linear approximation of the negative stiffness is not appropriate, non-linear function can be used. A fourth order polynomial function as shown in Eq. (3) is found to be suitable:

$$F_{sc} = V + W\Delta_f + X\Delta_f^2 + Y\Delta_f^3 + Z\Delta_f^4 \qquad (\Delta_f > \Delta_{max}) \tag{3}$$

where F_{sc} = Shear connection force
Δ_f = Displacement due to slip in shear connection

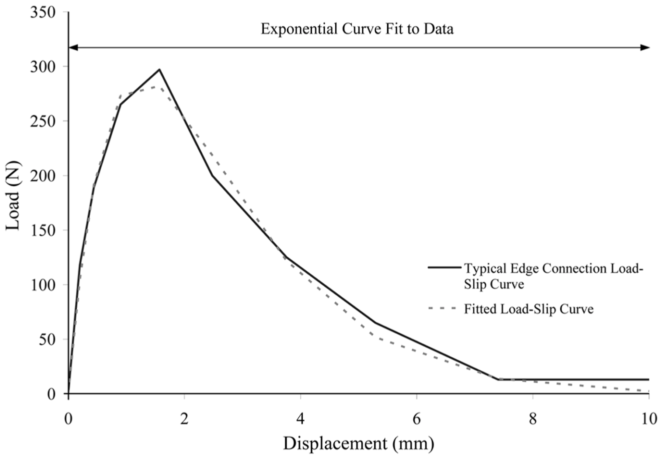

Fig. 8 An example of fitted load-slip curve for an edge shear connection

V, *W*, *X*, *Y* and *Z* are the variables obtained through fitting the data using a least squares regression method.

As depicted in Fig. 8, a typical load-slip curve of edge shear connections can be fitted using the following exponential function:

$$F_{sc} = A\Delta_f \exp(-B\Delta_f) \tag{4}$$

where F_{sc} = Shear connection force
Δ_f = Displacement due to slip in shear connection
A and *B* are the variables obtained through fitting the data using a least squares regression method.

5.2 Step 2: Obtain single stud deformation

Each single stud in a wall is assumed to have the ability to deform independently and the strain energy for each stud is additive to the overall strain energy of the wall, refer Section 4. Hence, a single stud model with the shear connections represented by springs, depicted in Fig. 9, can be used to establish a database for the deformations and bending energy of studs with different fastener spacing configurations as well as different types of plasterboard. Further, as shown previously in Fig. 6, studs in plasterboard clad walls deform symmetrically about mid height and plasterboard translate at half the stud deformation, only the top half of the stud was therefore considered in this single stud model and the hinge at mid height was represented by pin. Displacements caused by plasterboard translation, at this stage have also been included into the model.

To simplify the mathematical presentation, the following formulation is presented by temporarily assuming that the load-slip characteristics of the shear connections (springs) are linear elastic.

The total strain energy of the springs (Ω_f) on one stud can be written as:

$$\Omega_f = \sum_{i=1}^{n} \frac{1}{2} k_{f_i} \Delta_{f_i} \tag{5}$$

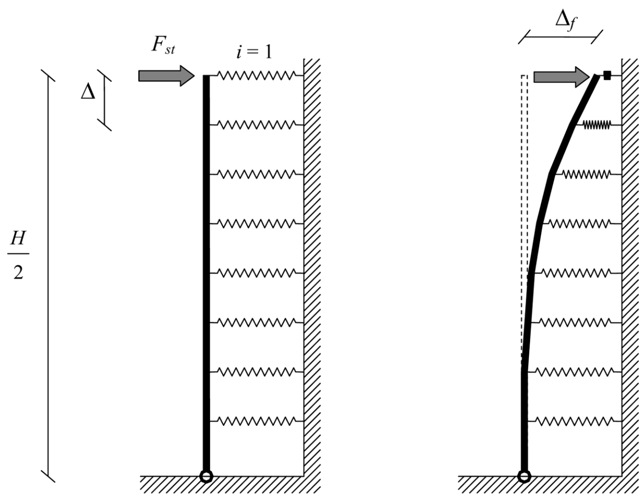

Fig. 9 Model of a single stud with shear connections represented by springs

where n = Number of springs on the stud
k_{f_i} = Stiffness of the spring i
Δ_{f_i} = Displacement due to slip in spring i

The bending strain energy (Ω_b) for a single stud can then be expressed in the following form using finite difference approximation:

$$\left.\begin{aligned}\Omega_b &= \frac{1}{2}EI\left(\frac{\Delta_{f_1} - 2\Delta_{f_2} + \Delta_{f_3}}{\Delta^2}\right)\frac{\Delta}{2} + \sum_{i=1}^{n-1}\frac{1}{2}EI\left(\frac{\Delta_{f_i} - 2\Delta_{f_{i+1}} + \Delta_{f_{i+2}}}{\Delta^2}\right)\Delta \\ &+ \frac{1}{2}EI\left(\frac{\Delta_{f_{n-1}} - 2\Delta_{f_n} + \Delta_{f_{n+1}}}{\Delta^2}\right)\frac{\Delta}{2}\end{aligned}\right\} \tag{6}$$

where n = Number of springs on the stud
Δ = Fastener spacing
E = Elastic modulus of the stud
I = Second moment of area of stud
Δ_{f_i} = Displacement due to slip in spring i

The total strain energy associated with a single stud thus becomes:

$$\Omega_s = \Omega_f + \Omega_b \tag{7}$$

The work done by the external force (W) is calculated as:

$$W = F_{st} \times \Delta_{f_1} \tag{8}$$

where F_{st} = Force applied to the tip of the stud
Δ_{f_1} = Displacement of first spring (where the force is applied)

As a result, the total potential energy in the system is given by:

$$P = \Omega_s - W \tag{9}$$

For the system to reach equilibrium when a force, F_{st}, or tip displacement, Δ_{f_1}, is applied, the stud will deform in such a way that minimum energy state is achieved. Thus, by differentiating P with respect to each spring deformation, Δ_{f_i}, the following equilibrium equations are obtained, for example:

Stud with n springs (where n > 5):

$$\left.\begin{aligned}
\frac{dP}{d\Delta_{f_i}} &= k_{f_1}\Delta_{f_1} + \frac{EI}{\Delta^3}\left(\frac{3}{2}\Delta_{f_1} - 3\Delta_{f_2} + \frac{3}{2}\Delta_{f_3}\right) - F = 0 \\
\frac{dP}{d\Delta_{f_2}} &= k_{f_2}\Delta_{f_2} + \frac{EI}{\Delta^3}(-3\Delta_{f_1} + 7\Delta_{f_2} - 5\Delta_{f_3} + \Delta_{f_4}) = 0 \\
\frac{dP}{d\Delta_{f_3}} &= k_{f_3}\Delta_{f_3} + \frac{EI}{\Delta^3}\left(\frac{3}{2}\Delta_{f_1} - 5\Delta_{f_2} + \frac{13}{2}\Delta_{f_3} - 4\Delta_{f_4} + \Delta_{f_5}\right) = 0 \\
\frac{dP}{d\Delta_{f_i}} &= k_{f_i}\Delta_{f_i} + \frac{EI}{\Delta^3}(\Delta_{f_{i-2}} - 4\Delta_{f_{i-1}} + 6\Delta_{f_i} - 4\Delta_{f_{i+1}} + \Delta_{f_{i+2}}) = 0 \\
&\vdots \\
\frac{dP}{d\Delta_{f_{n-1}}} &= k_{f_{n-1}}\Delta_{f_{n-1}} + \frac{EI}{\Delta^3}\left(\Delta_{f_{n-3}} - 4\Delta_{f_{n-2}} + \frac{13}{2}\Delta_{f_{n-1}} - 5\Delta_{f_n}\right) = 0 \\
\frac{dP}{d\Delta_{f_n}} &= k_{f_n}\Delta_{f_n} + \frac{EI}{\Delta^3}(\Delta_{f_{n-2}} - 5\Delta_{f_{n-1}} + 7\Delta_{f_n}) = 0
\end{aligned}\right\} \tag{10}$$

where i = 4, 5, 6 ... $n - 2$
n = Number of springs on the stud

The non-linearity of load-slip spring characteristics can now be reintroduced into Eq. (10) by replacing $k_f\Delta_f$ terms with the load-slip equations derived in Step 1 of this module (Module 1). Eq. (10) can be solved simultaneously through an iterative procedure to obtain the relationship between the deformation of the top spring (i = 1) and the deformation of each subsequent spring in the stud as well as the deformation of the stud. Concurrently, strain energy due to stud bending can be calculated using Eq. (6). As aresult, by utilising Eq. (5) to Eq. (10), a database, which comprises stud-spring deformations and stud bending energy that correspond to the top spring deformation for different fastener spacing configurations as well as for different types of plasterboard, is established. The database is then input into Module 2 of the MCFM model, which is described in detail in the next section. A comparison between the middle stud deformations at 5 mm intervals predicted by this single stud model and those obtained from the FE model is presented in Fig. 10. It can be seen from this figure that the single stud model predicts the stud deformations of Walls A and C with an excellent degree of accuracy.

It is important to point out that the MCFM model is far superior to the available closed-form

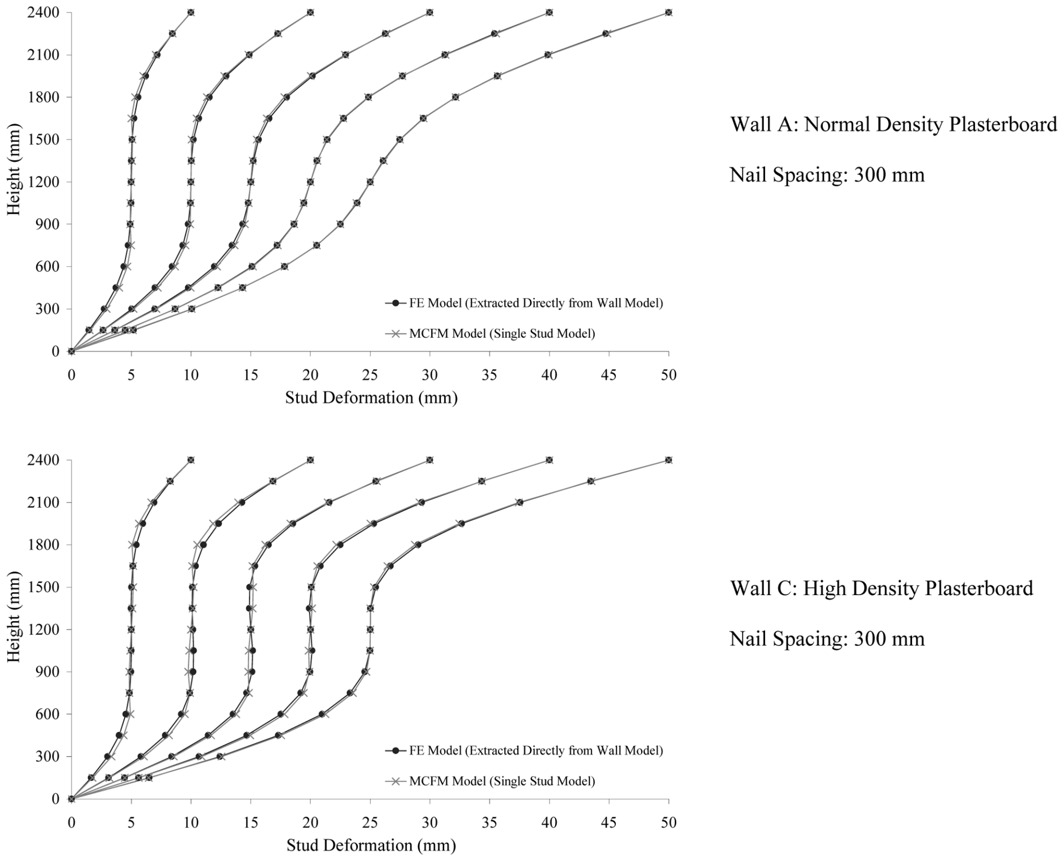

Fig. 10 Comparison between stud deformations obtained from the single stud model and the FE model

mathematical models which assume a certain function for stud deformations (e.g. sinusoidal function for S-shape stud deformations). The MCFM model generates the shape of the stud deformation based on the load-slip characteristics of shear connections and properties of studs (i.e. material and geometry of stud sections). Furthermore, the shape of the stud deformation is not constant as the relative stiffness between the stud bending and the shear connections varies due to non-linearity of their load-slip characteristics. Hence, unlike other closed-form mathematical models, users do not need to artificially constrain the stud deformations into a specific function.

6. Module 2: Solving for wall load-displacement response

This section presents a detailed description of the steps developed in this module for predicting the load-displacement response of plasterboard clad walls.

6.1 Step 1: Load-displacement response due to frame deformation and nail slip

In this step, the principle of conservation of energy is employed to obtain the load-displacement response of a wall due to frame deformation and nail slip. By utilising this principle where external work done (energy) is equal to internal strain energy, the total strain energy of the wall model at each specific frame displacement, Δ_F, is calculated and subsequently this energy is converted to the wall racking load, F_w. This process is displacement controlled where lateral displacement is applied at constant increments to the wall top plate.

The following lists the components which contribute to the internal strain energy of the wall model:

- Stud bending strain energy – This includes all the studs in the wall. The bending strain energy in each stud is assumed to be unique depending on the spacing of the fasteners and the location of the stud. Since all the studs in the wall are assumed to be connected by a rigid top plate, the deformation at the tip of each stud would be the same. The bending strain energy at each specific displacement can then be obtained from the database created in Module 1.
- Strain energy of shear connections on the top and bottom plates – Since these plates are assumed to be rigid, the slip of all the shear connections on each plate is equal to the applied frame displacement, Δ_F. In addition, due to the symmetry of the stud deformation, the shear connections at the top and bottom plates have the same deformation. Using numerical integration (e.g. Rectangular or Trapezoid Approximation and Simpson's Rule), the strain energy of the shear connections can then be calculated.
- Strain energy of shear connections on the studs – The slip of each shear connection can be acquired from the database created in Module 1. The strain energy of these shear connections can be calculated using numerical integration.

Next, the wall racking load (F_w) is calculated by converting the total strain energy of the wall into a rectangular area with its width equalling the incremental unit of the frame displacement (Δ_F) at each iteration and its height representing the corresponding racking load (F_w). Hence, the load-displacement response due to frame deformation and nail slip for the MCFM model can be derived through an iterative procedure.

6.2 Step 2: Additional displacement due to shearing of plasterboard

Similar to the procedure proposed by McCutcheon (1985), this step is designed to obtain the additional displacement caused by the shear deformation, Δ_{sh}, of the plasterboard. This displacement is then added to the incremental displacements applied in Step 1 to obtain the actual wall displacement, Δ_w. The shear deformation, Δ_{sh}, is calculated by assuming that the fasteners and the sheathings act in 'series' in resisting the racking load and the full racking force is transmitted through the fasteners into the plasterboard. As a result, the shear deformation of the plasterboard, Δ_{sh}, can be approximated by using the equation for the shear deformation of a thin, edge-loaded plate:

$$\Delta_{sh} = \frac{F_w H}{GtL} \tag{11}$$

where F_w = Racking load on wall
H = Height of the Wall
L = Length of the Wall
t = Thickness of plasterboard
G = Shear modulus of plasterboard

7. Computational algorithm

The database approach used in the MCFM modelling gives users the flexibility to extend the model to include different nailing patterns and load-slip characteristics of fastener connections as well as various types of plasterboard and timber cross-sections. Spreadsheets programs, such as Microsoft Excel which allows for automation in the computing process through the use of macro, suit well to the iterative nature of the algorithm of the MCFM model. The computation time for the final output (excluding creation of database in Module 1) takes several minutes for any reasonable number of deformation increments. The output includes an entire load-deformation curve and if necessary the characteristics parameters such as ultimate load and corresponding deflection can also be generated. Furthermore, other information such as secant or tangent stiffness at any point can be calculated.

8. Verification and applicability of MCFM model

Based on the formulation developed in the previous sections, the MCFM model was programmed into Microsoft Excel using Visual Basic. The model was then used to predict the load-displacement responses of Walls A to D as modelled using the FE model. The wall configurations are summarised in Table 1 and Fig. 11.

Table 1 Details of Walls A to D

	Plasterboard type	Nail spacing (mm)	
		Perimeter	Intermediate
Wall A	Normal density	150	300
Wall B	Normal density	300	300
Wall C	High density	150	300
Wall D	High density	300	300

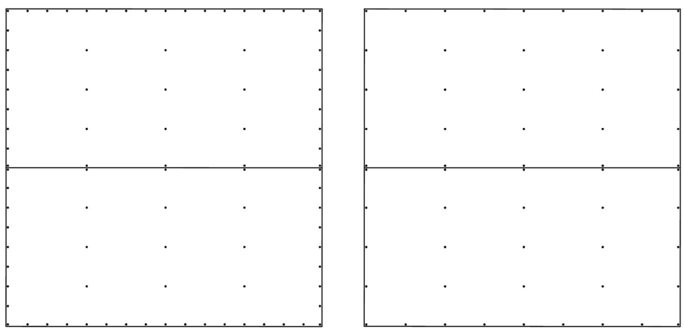

Wall A and Wall C

Wall B and Wall D

Note:
- All nails at the perimeter were fixed 15 mm away from the board edges.
- No nails were fixed on the noggings (standard practice in Australia)

Fig. 11 Nailing patterns of Walls S to V

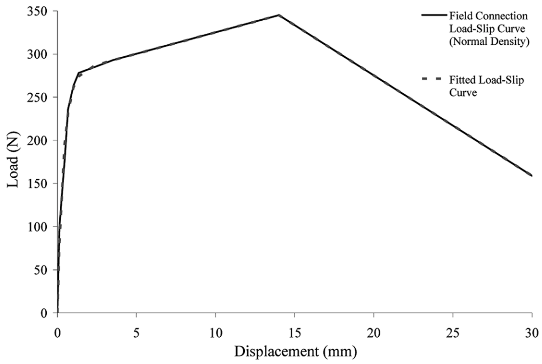

Field Connection (Normal Density)

Exponential Curve:

$$F = \left(A + B\Delta_f\right)\left(1 - \exp\left(-\frac{C}{A}\Delta_f\right)\right)$$

A = 275.49; B = 4.96; C= 731.02

Linear Regression:

$$F = M\Delta_f + N$$

M = -11.63; N = 507.75

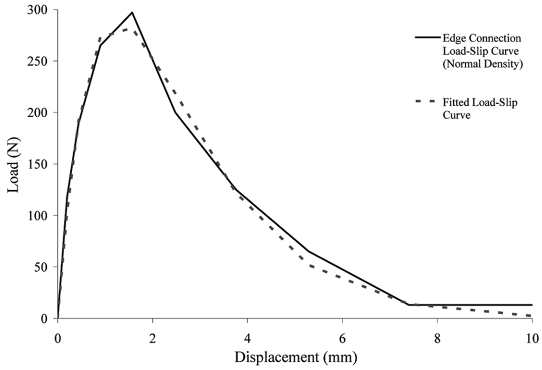

Edge Connection (Normal Density)

Exponential Curve:

$$F = A\Delta_f \exp(-B\Delta_f)$$

A = 613.60; B = 0.78

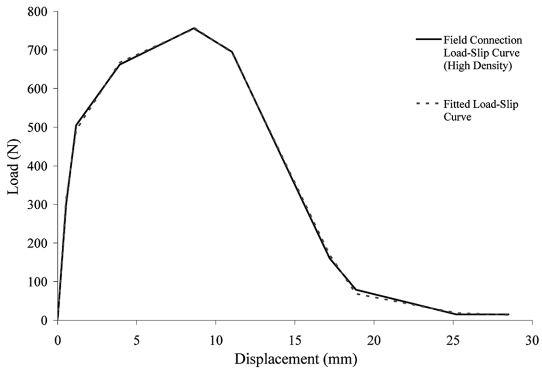

Field Connection (High Density)

Exponential Curve:

$$F = \left(A + B\Delta_f\right)\left(1 - \exp\left(-\frac{C}{A}\Delta_f\right)\right)$$

A = 600.78; B = 17.87; C= 808.12

Fourth Order Polynomial Curve:

$$F = V + W\Delta_f + X\Delta_f^{\,2} + Y\Delta_f^{\,3} + Z\Delta_f^{\,4}$$

V = -2565.83; W = 949.53; X = -91.42;
Y = 3.39; Z = -0.04

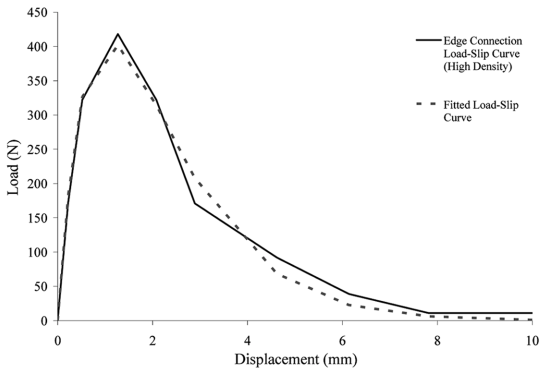

Edge Connection (Normal Density)

Exponential Curve:

$$F = A\Delta_f \exp(-B\Delta_f)$$

A = 1010.13; B = 0.91

Fig. 12 Summary of the resulting fitted load-slip curves for the field and edge shear connections

The key inputs to the MCFM model are as follows:

- Similar to the FE model, the wall dimensions and framing profile adopted in the MCFM model are the same as that of wall specimens tested in an experimental program. In other words, the dimension of each modelled wall was 2.4 m in height and length and consisted of a top plate, bottom plate and five studs with 600 mm centre to centre.
- For comparison purpose, the shear modulus (for plasterboard) and elastic modulus (for framing members) adopted in the MCFM model were the same as those applied in the FE model, that is, 724 MPa and 20 GPa, respectively.

A total of four types of shear connections were tested based on the shear connection test setup recommended by Liew *et al.* (2001) in order to represent the connections at the field and the edge studs as well as two different types of plasterboard (Normal Density and High Density). The original load-slip curves along with the fitted curves are presented in Fig. 12.

A comparison between the load-displacement responses of Walls A to D obtained from the MCFM model and those from the FE model is presented in Fig. 13. It can be seen from this figure that excellent agreement was achieved between the load-displacement curves predicted by the MCFM model and those by the FE model. It should be noted that the excellent agreement between the results of the MCFM and FE models is not limited only to overall wall the load-displacement response but also to the deformations of the frame and plasterboard. This level of accuracy is primarily attributed to the 'modularised' formulation described earlier.

To further verify the MCFM model, four additional walls were modelled with different nail spacing recommended by AS/NZS2589.1-1997 for adhesive/fastener fixing to timber framed walls but replacing adhesive with nails. Two different framing member sections were also adopted in these wall models. The dimensions of the studs and plates for the first wall (Wall E) and the second wall (Wall F) were 70 mm × 35 mm whereas the third wall (Wall G) and the fourth wall (Wall H) were 90 mm × 35 mm. The former section dimensions are normally used for internal walls of light-framed residential structures in Australia and the later is for external walls. Walls E to H were clad with normal density plasterboard. The details of the nail spacing and the section dimensions of these wall models are presented in Table 2.

Comparison between the resulting load-displacement curves of Walls E to F obtained from the MCFM model and FE model is shown in Fig. 14. Again, the MCFM model predicted the load-displacement curves of the walls with a very good degree of accuracy. Having performed the verifications of the load-displacement curves of plasterboard clad walls predicted by the MCFM model against those obtained from the FE model, the formulation of the MCFM model has proven to be accurate and representative. The MCFM model has also proven to be flexible to accommodate various nailing patterns and different framing member dimensions.

Table 2 Adopted framing member dimensions and nail spacing for Walls E, F, G and H

Wall	Timber section dimensions (mm)	Nail spacing (mm)		
		Edge studs	Plates	Intermediate studs
E	70 × 35	150	600	300
F	70 × 35	300	600	300
G	90 × 35	150	600	300
H	90 × 35	300	600	300

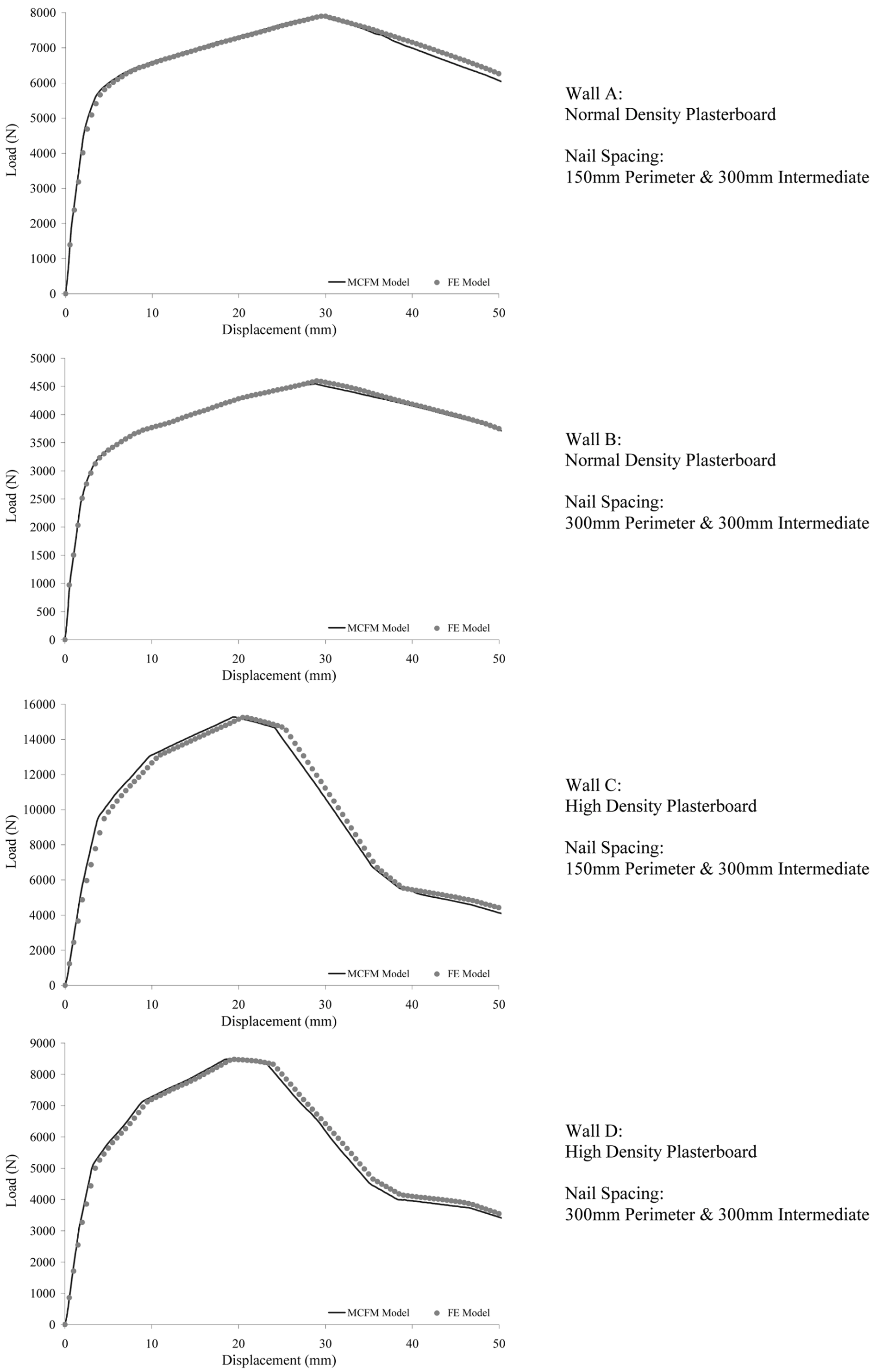

Fig. 13 Comparison between load-displacement curves obtained from the MCFM and the FE models, Walls A to D

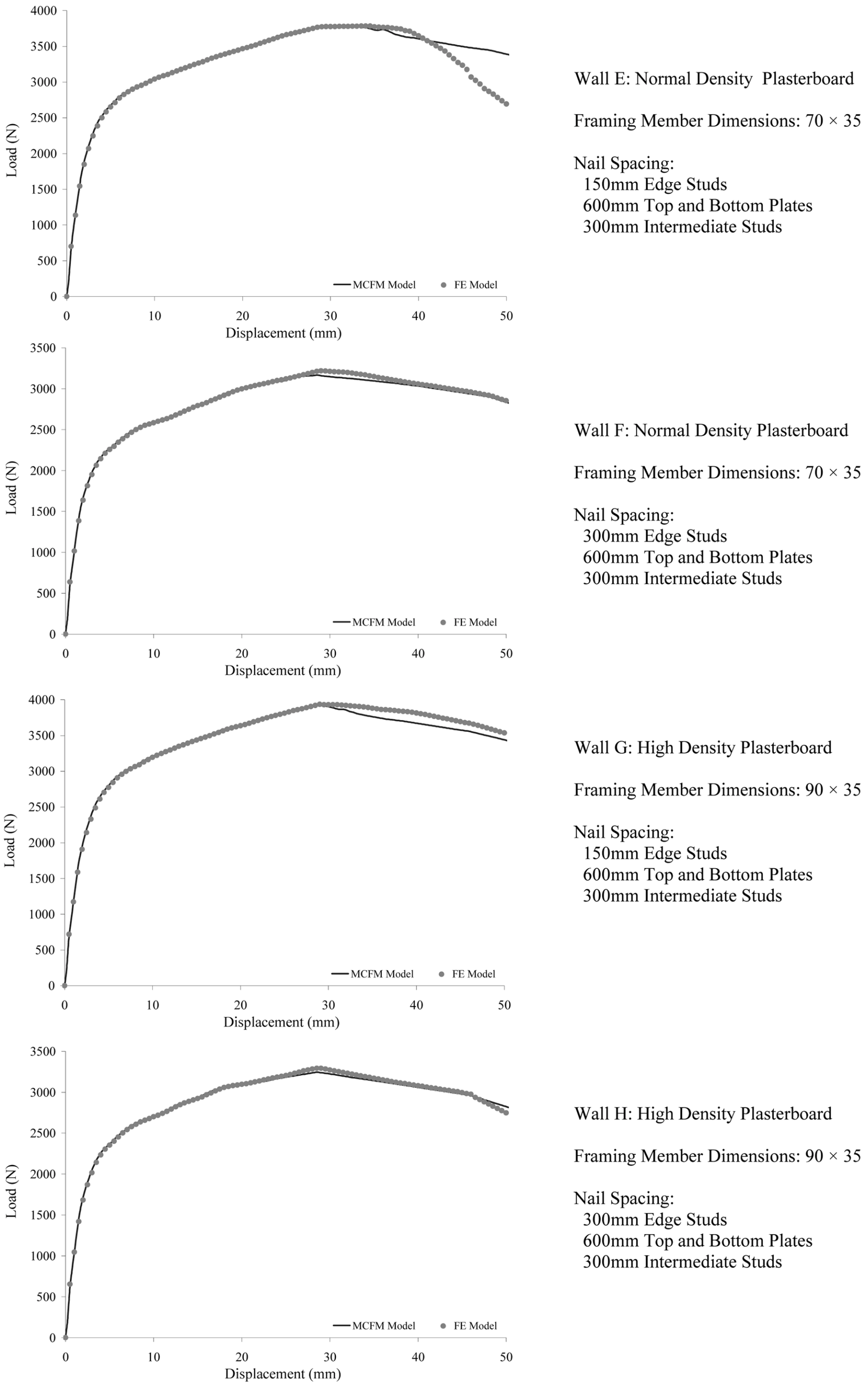

Fig. 14 Comparison between load-displacement curves obtained from the MCFM and the FE models, Walls E to H

Figs. 13 and 14 also show the influence of the various nailing spacing on the bracing performance of plasterboard clad walls. It can be seen from Fig. 14 that an increase in the framing member sections by about 25% did not have a significant effect on either the ultimate load or the load-displacement response of the wall. In addition, by comparing the results of Wall E and Wall F, a 100% increase in the nail spacing at the edge studs resulted in an approximately 20% decrease in the wall ultimate load. On the other hand, the results of Wall A (Fig. 13) and Wall E (Fig. 14) indicate that nail spacing at the top and bottom plates played a more significant role where a 100% increase in nail spacing decreased the wall ultimate load by almost 100%. Hence, it can be concluded that to attain higher bracing capacity for plasterboard clad walls, the most effective nailing pattern would be achieved by reducing the nail spacing at the plates.

9. Conclusions

The predictions generated by the MCFM model have been verified against the results obtained from the FE model and excellent agreement was reported. The MCFM model has also proven to be flexible in accommodating various nailing patterns and different framing member dimensions.

In summary, the following conclusions can be drawn from this analytical study:

- Strain energy due to stud deformation is significant and must be included in modelling of the plasterboard clad walls commonly found in light-framed residential structures in Australia.
- Deformation of each stud can be independent of the other studs in the wall and the strain energy of each stud is additive to the total internal strain energy of the wall subjected to racking load.
- The results of load-displacement responses predicted by the MCFM model matched remarkably well with that of the FE model.
- The MCFM model has the capability of assigning different load-slip characteristics for shear connections to account for the effects of the fastener locations on the wall which are particularly important for walls clad with plasterboard, where the shear connections at the cut edges of the plasterboard are substantially weaker than those at fielding the middle of the board (field).
- The MCFM model has established the basis for developing a spreadsheet-based program to analyse the load-displacement response for plasterboard clad walls. This fulfils the demand for straightforward and cost effective computer programs to perform the day-to-day design and calculation.
- The influence of the various nail spacing at the top and bottom plates is significant in providing bracing capacity for plasterboard clad wall. Changes in the framing member dimensions typically adopted in Australian light-framed structures, however, do not have much effect on the bracing performance of plasterboard clad walls.
- The MCFM closed form model provides an accurate estimate of the lateral capacity of plasterboard clad walls, typically constructed in Australia.

Acknowledgements

This study was carried out in the Department of Civil and Environmental Engineering at the University of Melbourne with financial support of ARC SPIRT Grant No. C89804857. The authors gratefully acknowledge the invaluable input of the research partners and their supportive staff of

Boral Australian Gypsum, CSR Building Materials and BHP Steel. Special thanks to the City of Mildura for providing M.K.N Johansen Memorial Scholarship to the first author.

Significant support has also been received from a number of collaborators and this support is also acknowledged. These collaborators are the helpful staff from CSIRO Building, Construction and Engineering, and the structures laboratory of The University of Melbourne.

References

Dolan, J.D. (1989), "The dynamic response of timber shear walls", thesis submitted in partial fulfilment of the requirements for the degree of Doctor of Philosophy, University of British Columbia.

Easley, J.T., Foomani, M. and Dodds, R.H. (1982), "Formulas for wood shear walls", *J. Struct. Div.*, ASCE, **108**(ST11), 2460-2478.

Folz, B. and Filiatrault, A. (2001), "CASHEW Version 1.0, A computer program for the cyclic analysis of shear walls", CUREE, Richmond, California.

Folz, B. and Filiatrault, A. (2002), "SAWS Version 1.0, A computer program for seismic analysis of woodframe structures" CUREE, Richmond, California.

Foschi, R.O. (1974), "The load-slip characteristics of nails", Department of the Environment, Canadian Forest Service, Western Forest Products Laboratory.

Foschi, R.O. (1977), "Analysis of wood diaphragms and trussess, Part one: Diaphragms", *Canadian J. Civil Eng.*, **4**(3), 345-352.

Gad, E.F. (1997), "Performance of brick-veneer steel-framed domestic structures under earthquake loading", thesis submitted in Total Fulfilment of the Requirements of the Degree of Doctor of Philosophy, Department of Civil and Environmental Engineering, The University of Melbourne.

Gad, E.F., Chandler, A.M., Duffield, C.F. and Stark, G. (1999), "Lateral behaviour of plasterboard-clad residential steel frame", *J. Struct. Eng.*, ASCE, **125**(1), 32-39.

Gupta, A.K. and Kuo, G.P. (1985), "Behaviour of wood-framed shear walls", *J. Struct. Eng.*, ASCE, **111**(8), 1722-1733.

Gutkowski, R.M. and Castillo, A.L. (1988), "Single and double-sheathed wood shear wall study", *J. Struct. Eng.*, ASCE, **114**(6 June), 1268-1284.

Itani, R.Y. and Cheung, C.K. (1984), "Nonlinear analysis of sheathed wood diaphragms", *J. Struct. Eng.*, ASCE, **110**(9), 2137-2147.

Kasal, B., Leichti, R.J. and Itani, R.Y. (1994), "Nonlinear finite element model of complete light frame wood structures", *J. Struct. Eng.*, ASCE, **120**(1), 100-119.

Liew, Y.L., Gad, E.F. and Duffield, C.F. (2001), "Assessment of plasterboard properties and relationship to lateral capacity of residential structures", *Proc. of the Australasian Structural Engineering Conf. 2001*, Gold Coast, Australia, 539-545.

Liew, Y.L., Gad, E.F. and Duffield, C.F. (2002), "Development of a method to control the bracing performance of plasterboard", *Proc. of the 17th Australasian Conf. on the Mechanics of Structures and Materials*, Gold Coast, Australia, 339-343.

McCutcheon, W.J. (1985), "Raking deformations in wood shear walls", *J. Struct. Eng.*, ASCE, **111**(2), 257-269.

Murakami, M., Moss, P.J., Carr, A.J. and Inayama, M. (1999), "Formulae to predict non-linear behaviour of sheathed walls with any nailing arrangement pattern", *Proc. of Pacific Timber Engineering Conf.*, Rotorua, New Zealand, 189-196.

Neisel, R.H. and Guerrera, J.F. (1956), "Racking strength of fiberboard sheathing", *Tappi J.*, **39**(9), 625-628.

Neisel, R.H. (1958), "Racking strength and lateral nail resistance of fiberboard sheathing", *Tappi J.*, **41**(12), 735-737.

Patton-Mallory, M. and McCutcheon, W.J. (1987), "Predicting racking performance of walls sheathed on both sides", *Forest Products J.*, **37**(9), 27-32.

Reardon, G.F. (1990), "Simulate cyclone wind loading of a Nu-Steel House", Technical Report No. 36, Cyclone Testing Station, James Cook University of North Queensland, Townsville, Australia.

Salenikovich, A.J. (2000), "The racking performance of light-frame shear walls", thesis submitted in partial fulfilment of the requirements for the degree of Doctor of Philosophy, Department of Wood Science and Forest Products, Virginia Polytechnic Institute and State University.

Standards Association of Australia (1992), *AS1684: National Timber Framing Code*.

Standards Association of Australia (1997), *AS/NZS2589.1: Gypsum Linings in Residential and Light Commercial Construction-Application and Finishing.*

Standards Association of Australia (1998), *AS/NZS2588: Gypsum Plasterboard*.

Standards Association of Australia (1999), *AS1684: Residential Timber-Framed Construction.*

Tuomi, R.L. and McCutcheon, W.J. (1978), "Racking strength of light-frame nailed walls", *J. Struct. Div.*, ASCE, **104**(ST7), 1131-1140.

Welsch, G.J. (1963), "Racking strength of half-inch fibreboard sheathing", *Tappi J.*, **46**(8), 458-465.

White, M.W. (1995), "Parametric study of timber shear walls", thesis submitted in partial fulfilment of the requirements for the degree of Doctor of Philosophy, Department of Wood Science and Forest Products, Virginia Polytechnic Institute and State University.

Glossary

Plasterboard: Also known as gypsum board, gypsum wallboard, gypsum panel and gypsum sheathing, the generic name for a family of sheet products consisting of non-combustible core primarily of gypsum with paper surfacing.

Shear Connection: This term is used to represent the connection between cladding material and frame via fastener. This is also commonly known as sheathing-to-framing connection.

Shear Connection Test: Also known as monotonic shear test and cladding-to-framing connection test. The purpose of this test is to obtain the performance characteristics such as strength, stiffness and load-deflection relationship of the cladding-to-framing connection.

Sheathing: There are several terminologies to describe the material used to cover wall studs in domestic structures (e.g. cladding, sheathing and lining). In Australia, the term lining is generally used to describe the material covering the interior side of the frames, while the term cladding is often used for exterior side. In the literature it is often found that the term cladding and sheathing are interchangeable. Cladding, sheathing and lining all perform essentially the same function, that is providing enclosure and possibly lateral bracing to the wall frames. Since this paper is concerned with lateral bracing of walls which can be due to cladding, sheathing or lining, these three terms will be used interchangeably.